

Supporting Information

Synthesis and catalytic activity of Pd doped Ni-MgO catalyst for dry reforming of methane

R. K. Singha,^a A. Shukla,^a A. Sandupatla,^b G. Deo,^b R. Bal*^a

^a Nanocatalysis Area, Conversions & Catalysis Division, CSIR-Indian Institute of Petroleum, Dehradun 248005, India. Fax: +91 135 2660202; Tel: +91 135 2525917.

^b Department of Chemical Engineering, Indian Institute of Technology Kanpur, Kanpur, 208016, India.

1. Characterization

The surface area analysis of the prepared samples were done at $-196\text{ }^{\circ}\text{C}$ with a Micromeritics ASAP 2020 (Micromeritics, GA, USA) using the BET equation. Degasification of the sample was done at $350\text{ }^{\circ}\text{C}$ for 6 h before analysis. Powder X-ray diffraction patterns of the samples were recorded on a Proto Analytical X-ray Diffraction System (AXRD) (PROTO Manufacturing, Ontario, Canada) fitted with a $\text{Cu K}\alpha$ radiation source. The X-ray diffraction patterns of all the samples were recorded in 10° – 80° region with a 0.04 step size (Dwell time = 1 s). Thermal stability of the catalysts, was checked from the XRD pattern of the after reaction catalyst compared with the XRD pattern of fresh catalyst. To check the reducibility of the catalysts, TPR experiments for the samples were carried out in a Micromeritics, Auto Chem II 2920 (Micromeritics, GA, USA) instrument connected with a thermal conductivity detector (TCD). TPR analysis for all the samples was done in the temperature range of 40 – $900\text{ }^{\circ}\text{C}$ with an increment of 10 K min^{-1} , using helium as carrier gas. Metal dispersion analyses of the catalysts were also carried out in a Micromeritics, Auto Chem II 2920 (Micromeritics, GA, USA) instrument connected with a thermal conductivity detector (TCD). SEM images of the prepared samples were taken on a FEI Quanta 200 F (FEI, Oregon, USA), using a tungsten filament doped with lanthanum hexaboride (LaB_6) as the X-ray source, fitted with an ETD detector with high vacuum mode, using secondary electrons and an acceleration tension of 10 or 30 kV. Analysis of the samples was done by spreading them on a carbon tape. Elemental analysis of the samples was carried out by energy dispersive X-ray spectroscopy (EDX). Distribution of all the elements of the catalyst was also checked by elemental mapping, using the same spectrophotometer. TEM images of the prepared samples were collected using a JEOL JEM 2100 microscope (JEOL, Tokyo, Japan). The samples were prepared by mounting an ethanol-dispersed sample on a lacey carbon Formvar coated Cu grid. Thermo Scientific K-Alpha X-ray photoelectron spectrometer

(Thermo Fisher Scientific, MA, USA) fitted with aluminium anode was used for X-ray photoelectron spectra (XPS) of the samples and binding energies (± 0.1 eV) were determined with the reference peak position of C 1s at 284.8 eV. The XPS spectra of the O 1s, C 1s, Ni 2p, Zn 2p regions were measured. Calibration of the binding energy (BE) scale was done by using the C 1s (BE = 284.6 eV) signal. TGA/DTG analysis of the prepared catalysts was carried out by the Perkin-Elmer TGA 4000 Thermogravimetric Analyzer (PerkinElmer, Massachusetts, USA).

2. Catalytic activity measurement

DRM was carried out in a fixed-bed down flow reactor at atmospheric pressure. Before reaction, all the catalysts were reduced at 500 °C for 2 h in presence of 20% H₂ balanced He gas. Typically, 60 mg of catalyst (mixed with catalytically inactive diluents, where catalyst to diluent ratio (w/w) was 1:5) was placed in between two quartz wool plugged in the centre of the 6 mm quartz tube reactor. DRM was carried out at different temperature (400-800 °C). The weight hourly space velocity (WHSV) was varied between 10000 mlg⁻¹h⁻¹ to 200000 mlg⁻¹h⁻¹ with a molar ratio of CH₄:CO₂:He of 1:1:12. The reaction products were analysed using an online gas chromatography (Agilent 7890A) (Agilent Technologies, California, USA) fitted with a TCD detector using two different columns Molecular sieves (for analysing H₂) and PoraPack-Q (for analysing CH₄, CO₂ and CO).

$$X_{CH_4}(\%) = [(F_{CH_4;in} - F_{CH_4;out}) \div F_{CH_4;in}] \times 100$$

$$X_{CO_2}(\%) = [(F_{CO_2;in} - F_{CO_2;out}) \div F_{CO_2;in}] \times 100$$

Where, $X_{CH_4}(\%)$ and $X_{CO_2}(\%)$ are the conversion of methane and CO₂. $F_{CH_4;in}$, $F_{CH_4;out}$ are the inlet and outlet flows of methane. $F_{CO_2;in}$, $F_{CO_2;out}$ are the inlet and outlet flows of CO₂.

3. Additional characterizations and reaction data

3.1. Scanning Electron Microscopic (SEM) analysis

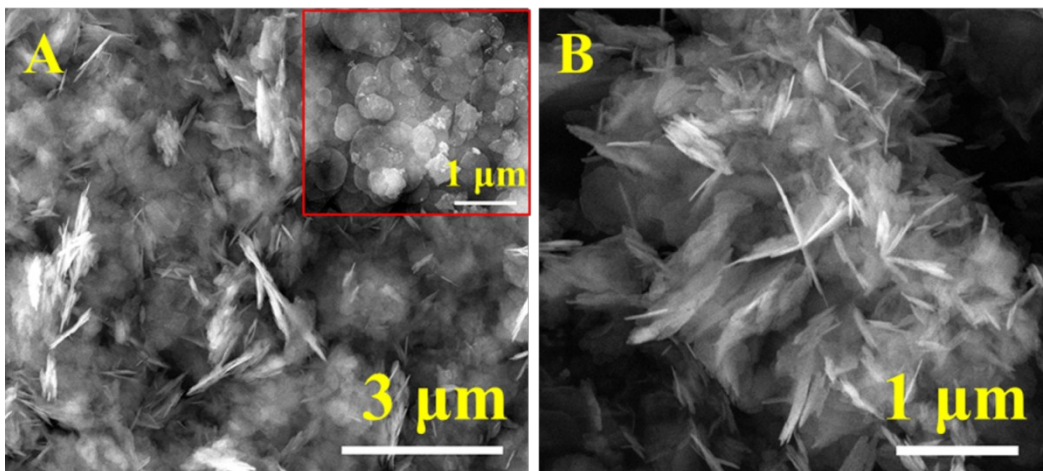


Figure S1: SEM images of (a) support MgO, (b) 0.2Pd/5Ni-MgO^F catalyst.

Morphological analysis of support MgO and 0.2Pd/5Ni-MgO^F catalyst was carried out by SEM images. Obtained results showed flakes and spherical sheets like morphology of prepared support MgO and 0.2Pd/5Ni-MgO^F catalyst.

3.2. XPS analysis of 5Ni-MgO^S catalyst

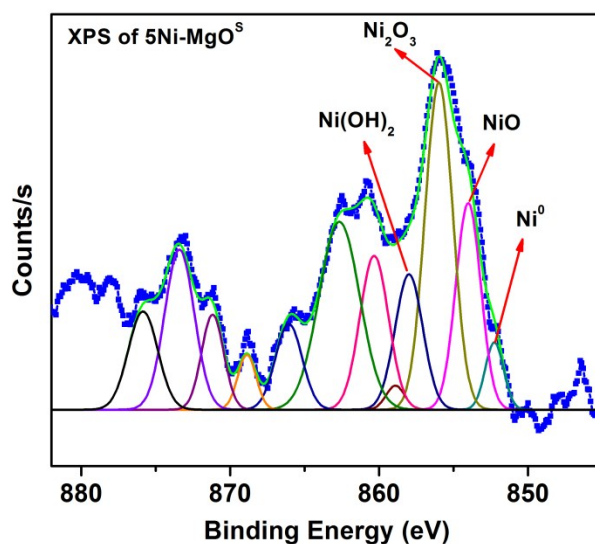


Figure S2: Ni2p core level spectra of 5Ni-MgO^S catalyst. **Spent catalyst condition:** Temperature (750 °C), Pressure (1 atm.), WHSV (70000 mlg⁻¹h⁻¹), Reaction time (100 h), Feed ratio (CH₄:CO₂:He = 1:1:12).

3.3. Optimization of Pd-doping

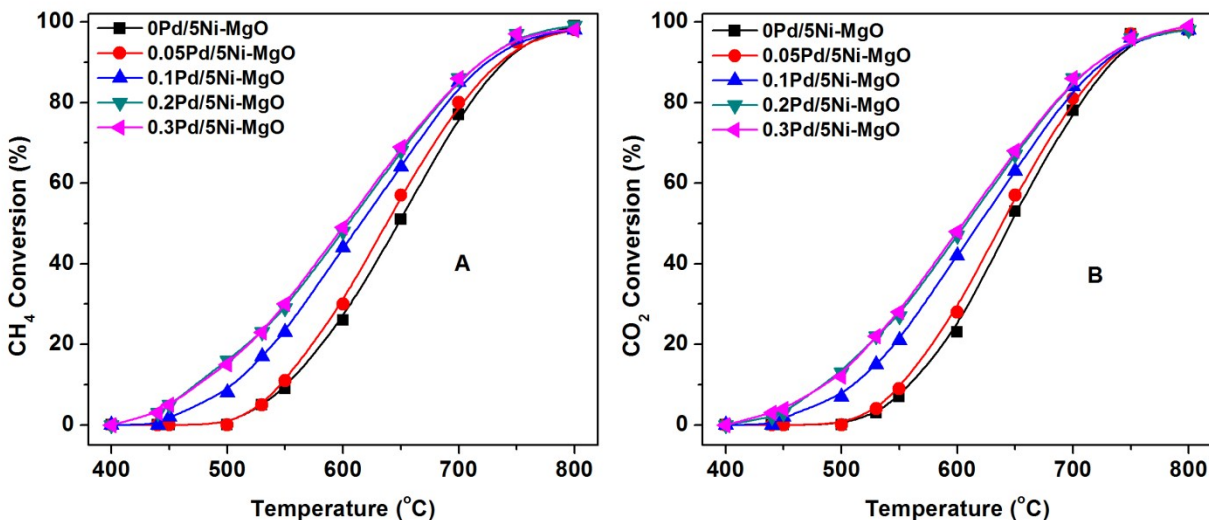


Figure S3: (A) Methane and (B) CO₂ conversions as a function of Pd-doping and temperature. **Reaction condition:** Temperature (400-800 °C), Pressure (1 atm.), WHSV (70000 mlg⁻¹h⁻¹), Feed ratio (CH₄:CO₂:He = 1:1:12).

3.4. Heat transfer and mass transfer (HT-MT) limitations

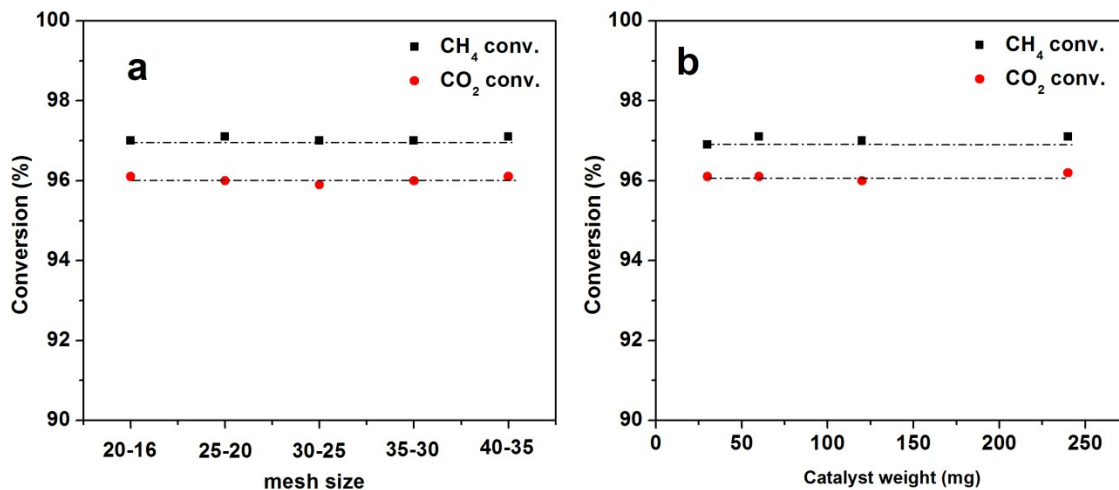


Figure S4. Reactant conversions using (a) different mesh size of catalyst and (b) different catalyst weight. **Reaction condition:** Temperature (400-800 °C), Pressure (1 atm.), WHSV (70000 mlg⁻¹h⁻¹), Feed ratio (CH₄:CO₂:He = 1:1:12).

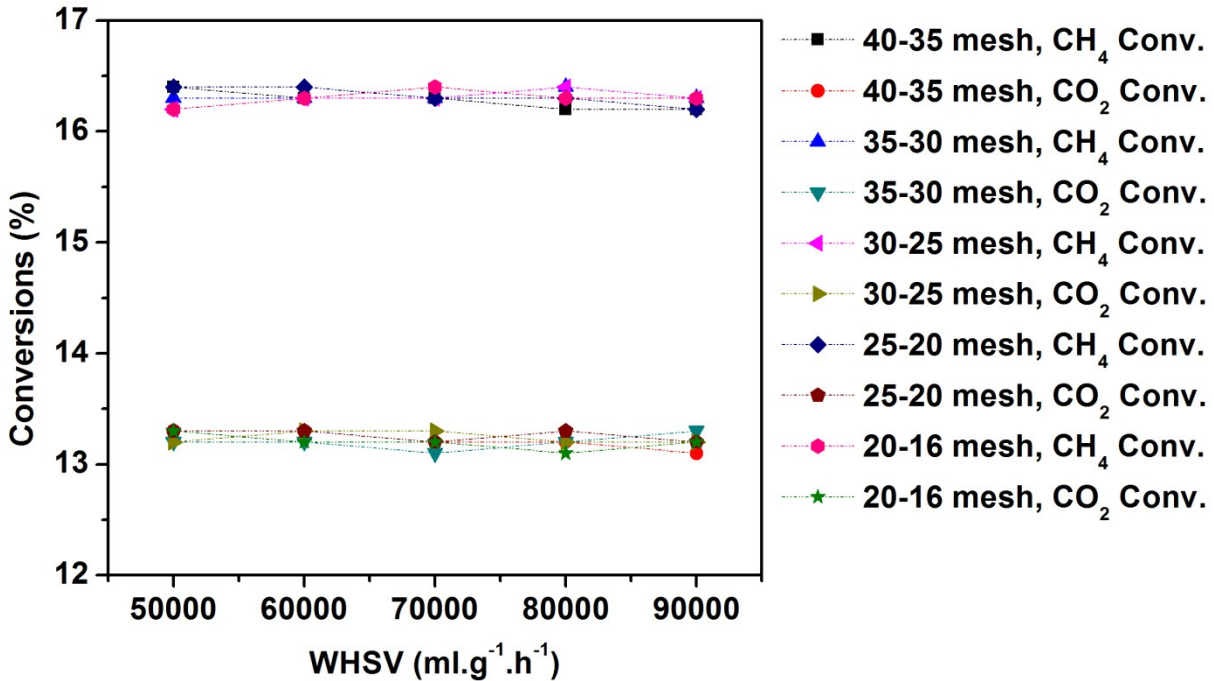


Figure S5. Effect of pellet size and WHSV.

Reaction condition: catalyst (60 mg) diluted with ground quartz, Temperature (500 °C), CH₄ : CO₂ : He = 1:1:12 (feed ratio), Pressure (1 atm.).

Heat transfer and mass transfer (HT-MT) limitations were checked for the DRM reaction over 0.2Pd/5Ni-MgO catalyst and it is presented in Figure S4, S5. HT-MT limitation is a major problem which the researchers face during catalysis for methane reforming reactions. In our case we have found that variation of mesh size of the catalyst and catalyst weight has minimal effect on reactants conversions, which indicated negligible HT-MT limitations.

Mass and Heat Transfer Calculations for Dry reforming of methane upon 0.2Pd/5Ni-MgO^F catalyst at 450 °C

For PBR reaction mode (7.14 CH₄ / 7.14 CO₂ / 85.71He) with respect to Methane

Mears Criterion for External Diffusion

If $\frac{-r_A' \rho_b R n}{k_c C_{Ab}} < 0.15$, then external mass transfer effects can be neglected.

$-r_A'$ = reaction rate, kmol/kg-cat · s = 3.1002×10^{-06}

n = reaction order = 1.3

R = catalyst particle radius, m = 5.3×10^{-5}

ρ_b = bulk density of catalyst bed, kg/m³ = 947

= (1- ϕ) (ϕ = porosity or void fraction of packed bed)

ρ_c = solid catalyst density, kg/m³ = 3.87×10^3

C_{Ab} = bulk gas concentration of A, kmol/m³ = 0.02962

k_c = mass transfer coefficient, m/s = 1.02 m/s

$$\frac{-r'_A \rho_b R n}{k_c C_{Ab}} = [3.1002 \times 10^{-06} \text{ kmol-C}_3/\text{kg-cat.s} \times 1000] [947 \text{ kg/m}^3] [5.3 \times 10^{-5} \text{ m}] [1.3] / ([1.02 / \text{s}] \times [0.02962 \text{ kmol/m}^3]) = \mathbf{6.70 \times 10^{-3} < 0.15 \text{ \{Mears for External Diffusion\}}}$$

Weisz-Prater Criterion for Internal Diffusion

If $C_{WP} = \frac{-r'_{A(\text{obs})} \rho_c R^2}{D_e C_{As}} < 1$, then internal mass transfer effects can be neglected.

$-r'_{A(\text{obs})}$ = observed reaction rate, kmol/kg-cat · s

R = catalyst particle radius, m

ρ_c = solid catalyst density, kg/m³;

D_e = effective gas-phase diffusivity, m²/s

$$= \frac{D_{AB} \phi_p \sigma_c}{\tau} \text{ where}$$

D_{AB} = gas-phase diffusivity m²/s; ϕ_p = pellet porosity; σ_c = constriction factor; τ = tortuosity.

C_{As} = gas concentration of A at the catalyst surface, kmol-A/m³

$$C_{WP} = \frac{-r'_{A(\text{obs})} \rho_c R^2}{D_e C_{As}} = [3.1002 \times 10^{-06} \text{ kmol-C}_3/\text{kg-cat.s} \times 1000] \times [3.87 \times 10^3 \text{ kg-cat/m}^3] \times [5.3 \times 10^{-5} \text{ m}]^2 / ([3.95 \times 10^{-6} \text{ m}^2/\text{s}] \times [0.02962 \text{ kmol-C}_3/\text{m}^3]) = \mathbf{2.88 \times 10^{-1} < 1}$$

\{Weisz-Prater Criterion for Internal Diffusion\}

Mears Criterion for External (Interphase) Heat Transfer

$$\left| \frac{-\Delta H_r (-r_A') \rho_b R E}{h_t T_b^2 R_g} \right| < 0.15$$

$$[258.8 \text{ kJ/mol} \times 3.1002 \times 10^{-06} \text{ kmol/kg-cat.s} \times 1000 \times 947 \text{ kg-cat/m}^3 \times 5.3 \times 10^{-5} \text{ m} \times 96.7 \text{ kJ/mol}] / [5.325 \text{ kJ/m}^2 \cdot \text{K.s} \times 723^2 \text{ K}^2 \times 8.314 \times 10^{-3} \text{ kJ/mol.K}] = 1.68 \times 10^{-4} < 0.15$$

{Mears Criterion for External (Interphase) Heat Transfer}

Mears Criterion for Combined Interphase and Intraparticle Heat and Mass Transport (Mears, 1971)

$$\frac{-r_A' R^2}{C_{Ab} D_e} < \frac{1 + 0.33 \gamma \chi}{n - \gamma_b \beta_b (1 + 0.33 n \omega)}$$

$$\gamma = \frac{E}{R_g T_s}; \gamma_b = \frac{E}{R_g T_b}; \beta_b = \frac{(-\Delta H_r) D_e C_{Ab}}{\lambda T_b}; \chi = \frac{(-\Delta H_r) - r_A' R}{h_t T_b}; \omega = \frac{-r_A' R}{k_c C_{Ab}}$$

γ = Arrhenius number; β_b = heat generation function;

λ = catalyst thermal conductivity, W/m.K;

χ = Damköhler number for interphase heat transport

ω = Damköhler number for interphase mass transport

$$\frac{-r_A' R^2}{C_{Ab} D_e} = [3.1002 \times 10^{-06} \text{ kmol/kg-cat.s} \times 1000 \times (5.3 \times 10^{-5})^2 \text{ m}^2] / [0.02962 \text{ kmol/m}^3 \times 3.95 \times 10^{-6} \text{ m}^2/\text{s}] = 7.44 \times 10^{-5} < 3$$

{Mears Criterion for Interphase and Intraparticle Heat and Mass Transport}

For PBR reaction mode (7.14 CH₄ / 7.14 CO₂ / 85.71He) with respect to CO₂

Mears Criterion for External Diffusion

$$\frac{-r_A' \rho_b R n}{k_c C_{Ab}} = [1.9221 \times 10^{-06} \text{ kmol-C}_3/\text{kg-cat.s} \times 1000] [947 \text{ kg/m}^3] [5.3 \times 10^{-5} \text{ m}] [1.5] / ([1.02 / \text{s}] \times [0.02962 \text{ kmol/m}^3]) = 4.79 \times 10^{-3} < 0.15 \text{ {Mears for External Diffusion}}$$

Weisz-Prater Criterion for Internal Diffusion

$$C_{WP} = \frac{-r'_{A(obs)} \rho_c R^2}{D_e C_{As}} = [1.9221 \times 10^{-06} \text{ kmol-C}^3/\text{kg-cat.s} \times 1000] \times [3.87 \times 10^3 \text{ kg-cat/m}^3] \times [5.3 \times 10^{-5} \text{ m}]^2 / ([3.95 \times 10^{-6} \text{ m}^2/\text{s}] \times [0.02962 \text{ kmol-C}^3/\text{m}^3]) = \mathbf{1.79 \times 10^{-1} < 1}$$

{Weisz-Prater Criterion for Internal Diffusion}

Mears Criterion for External (Interphase) Heat Transfer

$$\left| \frac{-\Delta H_r (-r'_A) \rho_b R E}{h_i T_b^2 R_g} \right| < 0.15$$

$$[258.8 \text{ kJ/mol} \times 1.9221 \times 10^{-06} \text{ k mol/kg-cat.s} \times 1000 \times 947 \text{ kg-cat/m}^3 \times 5.3 \times 10^{-5} \text{ m} \times 99.8 \text{ kJ/mol}] / [5.325 \text{ kJ/m}^2.\text{K.s} \times 723^2 \text{ K}^2 \times 8.314 \times 10^{-3} \text{ kJ/mol.K}] = \mathbf{1.08 \times 10^{-4} < 0.15}$$

{Mears Criterion for External (Interphase) Heat Transfer}

Mears Criterion for Combined Interphase and Intraparticle Heat and Mass Transport (Mears, 1971)

$$\frac{-r'_A R^2}{C_{Ab} D_e} < \frac{1 + 0.33\gamma\chi}{|n - \gamma_b \beta_b| (1 + 0.33n\omega)}$$

$$\gamma = \frac{E}{R_g T_s}; \gamma_b = \frac{E}{R_g T_b}; \beta_b = \frac{(-\Delta H_r) D_e C_{Ab}}{\lambda T_b}; \chi = \frac{(-\Delta H_r) - r'_A R}{h_i T_b}; \omega = \frac{-r'_A R}{k_c C_{Ab}}$$

γ = Arrhenius number; β_b = heat generation function;

λ = catalyst thermal conductivity, W/m.K;

χ = Damköhler number for interphase heat transport

ω = Damköhler number for interphase mass transport

$$\frac{-r'_A R^2}{C_{Ab} D_e} = [1.9221 \times 10^{-06} \text{ kmol/kg-cat.s} \times 1000 \times (5.3 \times 10^{-5})^2 \text{ m}^2] / [0.02962 \text{ kmol/m}^3 \times 3.95 \times 10^{-6} \text{ m}^2/\text{s}] = \mathbf{4.61 \times 10^{-5} < 3}$$

{Mears Criterion for Interphase and Intraparticle Heat and Mass Transport }